ESA Contract no. 4000116423/15/NL/BJ/gp

Optical Compressive Sensing (CS) Technologies for Space Applications (OCS-TECH)

Title:	Executive Summary			
Document Id:	FD2			
	Name:	Position:	Affiliation:	
Authors:	Stefano Baronti	Participant	CNR - IFAC	
	Andrea Donati	Participant	CNR - IFAC	
	Donatella Guzzi	Participant	CNR - IFAC	
	Cinzia Lastri	Participant	CNR - IFAC	
	Vanni Nardino	Participant	CNR - IFAC	
	Lorenzo Palombi	Participant	CNR - IFAC	
	Ivan Pippi	Participant	CNR - IFAC	
	Valentina Raimondi	PI	CNR - IFAC	
	Giulio Coluccia	Participant	POLI-TO	
	Enrico Magli	POLI-TO resp.	POLI-TO	
	Chiara Ravazzi	Participant	POLI-TO, presently at CNR-IEIIT	
	Mihaela Bojan	Participant	CEOSPACETECH	
	Daniela Coltuc	CEOSPACE resp.	CEOSPACETECH	
	Cristian Damian	Participant	CEOSPACETECH	
	Florin Garoi	Participant	CEOSPACETECH	
	Iuliana Iordache	Participant	CEOSPACETECH	
	Catalin Logofatu	Participant	CEOSPACETECH	
	Mihai Petrovici	Participant	CEOSPACETECH	
	Adrian Sima	Participant	CEOSPACETECH	
	Cristian Udrea	Participant	CEOSPACETECH	
	Alessandro Barducci	SOFASI resp.	SOFASI	
	Demetrio Labate	LEONARDO resp.	LEONARDO	
	Carlo Pompei	Participant	LEONARDO	
	Samuele Grella	Participant	LEONARDO	
Verified by:	Valentina Raimondi	PI	CNR - IFAC	
Approved by:	Valentina Raimondi	PI	CNR - IFAC	
Issued:	xxx			

1 INTRODUCTION

Shannon-Nyquist theorem rules the signal sampling stating that the signal must be sampled at a rate of at least twice the maximum frequency present in the signal to be fully reconstructed. Compressive Sensing (CS) theory affirms that a sparse signal can be efficiently reconstructed by the acquisition of a number of samples far below the minimal one dictated by Nyquist theorem, thus providing a new approach to data acquisition.

CS technique is based on the concept of sparsity. The information rate of a continuous "sparse" signal may be much smaller than suggested by its bandwidth. The benefit of CS is that it permits to design efficient sensing or sampling protocols that capture the useful information content embedded in a sparse signal and compact it into a small amount of data. A basic example of sparsity is constituted by a multidimensional signal with a strong average spatial and/or spectral autocorrelation, and hence a redundant representation. A mathematical representation, usually a linear transform, of the sparse signal exists in which the number of non-zero coefficients is less than the one in the original representation. The sparse representation is not employed during acquisition, but only during image reconstruction, and it enables signal reconstruction provided that the signal measurements have been acquired using random projections. When radiometric and spectroscopic signals are considered, an optical subsystem would be the natural choice for optically computing such random projections.

CS approach enabled the development of some novel instruments, such as the single pixel camera developed by the Rice University. On the basis of a time-multiplexing technique, a single-pixel camera is able to acquire an image using a single photodetector element instead of an array of detectors. Such approach is particularly important when there are no detector matrices available in the desired wavelength range.

The major advantages that could be expected from implementing optical CS-based instrumentation are:

- miniaturization of the system and simplification of the architecture;
- inherent compression of data;
- optimal selection and optimization of single pixel detectors for the selected application;

Several space applications could benefit from this technique, such as imaging, spectro-imagery and hyperspectral instruments for Earth Observation, Planetary Exploration and Space Science missions.

The objectives of the OCS-Tech project were:

- To investigate and assess the potential of using CS technologies in future optical instruments for some space applications, and to compare them with traditional systems.
- To design a CS based optical system (at elegant breadboard level) targeting a specific space application and targeting a significant advantage with respect to a traditional counterpart.

The project' activities required the collaboration of five teams with different expertise, from optical design and sensor's development and test, to CS signal processing. Table 1 summarizes the Institutions contributing to the project:

Table 1- The OCS -Tech partnership.

Institution	Project Role
IFAC-CNR(Main contractor)	Optical Instrument Design and Critical Evaluation
Politecnico di Torino (Sub contractor)	Performance Models and Evaluation
Leonardo SPA (Sub contractor)	Budget Assessment and Qualification
CEO (Sub contractor)	NIR to THz Expertise and Technical Support
SOFASI srl (Sub contractor)	Test Setup and Procedures

The project activities were organised in four main Work Packages (WP):

- WP1 was devoted to a detailed analysis of those space applications and optical systems that could potentially benefit from the use of CS techniques and relevant technologies.
- WP2 was devoted to the preliminary design of the two selected configurations and to the analysis of their performance on the basis of a preliminary performance model developed taking into account the main system parameters.
- WP3 was devoted to the detailed design of one of the two configurations and to the detailed analysis of its performance on the basis of an updated performance model.
- WP4 was devoted to the critical evaluation of the detailed design and performance estimations and to outline a detailed road-map of the activities needed for the development of an Engineering Model. The roadmap included also a schedule and a development cost estimate range. Recommendations for the development activities in order to reduce the criticality and to provide confidence in the proposed implementation were finally given.

2 STATE OF THE ART

A review of the current and future ESA missions in the field of Space Science (SS), Earth Observation (EO) and Planetary Exploration (PE) was performed, focusing particularly on those missions and instrumentation that are under development or are foreseen in the near future. Several instruments that could in principle benefit from CS paradigm were found. This review was followed by the analysis of the state of art of CS-based instrumentation implemented up to now including also the interesting spectral regions of the THz and microwaves. An analysis of the state of the art of the algorithms used for image reconstruction was also performed, together with a review of the critical components and relevant technologies. The critical components of a CS based system are mainly the spatial light modulator (SLM) and the detector. Presently, there are three types of SLMs on the market: Digital Micromirrors Arrays (DMD), Micro-Shutter Arrays (MSA), and Liquid Crystal Plate (LCP). While DMD and MSA have been tested for radiation, LCPs have not yet been tested. The other key element in CS architecture is the detector, which physically performs the integration in the transform domain. Detector is a less critical component with respect to the SLM, although high speed detectors are usually requested. Single pixel detectors that can be used for CS applications are the following:

- Silicon Photodiodes (from X-ray to Near InfraRed (NIR))
- Silicon Photomultiplies (from X-ray to NIR)
- Avalanche Photo Detectors (APDs)(from visible (VIS) to Medium InfraRed (MIR))
- InGaAs Photodiodes (Short Wave InfraRed (SWIR))
- InSb detectors (MIR)
- Photomultipliers (VIS-NIR)
- MCT Photodiodes (from VIS up to 10 micron)
- Pyroelectric Detector
- THz receivers.

In a CS-based instrument, N-pixel detectors can be replaced with a single-pixel detector. This can be achieved if, during the specified integration time, it is possible to perform a number of measurements $p*N$, with p usually ranging from 0.1 to 0.5. The p parameter is chosen according to the required data quality. Both the SLM switching speed and the detector frame rate are key parameters to obtain a good data quality.

The computational burden of reconstruction algorithms depend on the number of pixels N to be reconstructed for each image. In some cases, there are image dimensions for which the time needed to reconstruct the signal of interest can become so excessively long as to be of no practical use. Reconstruction time depends also on the type of algorithm employed for the reconstruction.

Generally, slower algorithms guarantee better results in terms of image quality.

3 PROPOSED CS-BASED INSTRUMENT CONCEPTS

The outcomes of the survey carried out in the first phase of the project were used to outline a number of CS-based instrument concepts. The latter are divided into two groups: the first one is devoted to CS-based instruments based on a classical approach to CS, relying on a full reconstruction of the image/signal; the second one is devoted to CS-based instruments based on a novel approach, relying on the extraction of the useful information rather than on a full reconstruction of the image/signal. All the proposed instrumental concepts are based on single pixel camera configuration. The list of the proposed instrument concepts contains the application field, the working spectral range and an overall ranking. This ranking was achieved by simply adding the values assigned to the following parameters:

- Total mass reduction
- Total power reduction
- Computational burden
- Compression ratio
- Data quality ("Information Content Accuracy" for the novel concepts)
- Cost reduction
- Integration time (multiplied by -1: scores were from 1 for not critical to 3 for very critical).

All these parameters, except for the integration time, were evaluated with respect to the corresponding traditional instrument. The ranking value range was set so that the higher was the score the better was the expected performance of the instrument concept in terms of budgets, data quality and development cost.

The expected data quality was assessed on the basis of data sparsity. Sparsity was evaluated in the pixel domain and in the DCT domain. For 2D images, the 2D DCT was evaluated. For 3D images, the 3D DCT was evaluated, on x-y, x-λ and y-λ planes. Sparsity was evaluated as the ratio k/N, where k is the total number of coefficients in a given domain and N is the number of sorted coefficients in that domain including the 99% of the signal energy.

The final ranking for the classical CS based instrumental concepts is reported in Table 2. Since for some instruments there was not information available in the literature on the total mass and power, or these were not reasonably predictable, two different final ranking lists were given, one based on total budgets and one on partial budgets. The partial budgets, in fact, included only a limited number of elements, specifically: the detection system, cryocooler, modulator (including focussing optics) and compression board.

The final ranking for the novel CS based instrumental concepts (Table 3) did not take into account the 'Information content accuracy' parameter since this parameter was not available for all the concepts. Furthermore, the final ranking was calculated by considering the partial mass and power consumption reduction with the exception of the two configurations working in the THz range for which only data referring to total budgets were available.

After a preliminary screening of all the proposed configurations and relevant scoring, the concepts identified as the most promising were highlighted as blue text in the two tables.

The selection of the most promising configurations was performed on the basis of: the overall score awarded in the final ranking tables, the overall technological maturity, and the score assigned to the most critical parameters, such as integration time and data quality.

Other considerations were also taken into account, such as the specific application and the platform used. Due to ESA policies for next future missions, configurations for rover platforms were considered of less interest.

Table 2 – Classical CS-based instruments (standard CS approach).

Conf. #	Short description	Field	Spectral range	Number of pixels	Integration time (1→3)	TRL HW	TRL SW	Mass reduction % (-2→ +2)	Power reduction % (-2→ +2)	Partial mass red. % (-2→ +2)	Partial power red. % (-2→ +2)	Comp. burden (-2→ +2)	Compression ratio (-2→ +2)	Data Quality (-2→ +2)	Cost reduction (-2→+2)	Final ranking (tot.budgets)	Final ranking (part.budgets)
1A	**UV-SWIR hyperspectral imager with tunable filters or dispersive elements on rover**	PE	UV - SWIR	512x256	1	4	4	+2	+1	+2	+2	-2	-1	-1	+2	0	1
2A	**UV-MIR hyperspectral imager with tunable filters or dispersive elements on orbiter**	PE	UV-MIR	432x256	2	4	4	+1	+2	+2	+2	-2	-1	-1	+2	-1	0
3A	UV-VIS optical camera with extended sensitivity on rover	PE	UV-Vis	512x512	1	4	4	+2	-2	+2	-2	-1	-2	-2	+1	-5	-5
4A	EUV camera on orbiter	SS	EUV	512x512	1	3	4	+1	-2	+2	-2	-2	-1	-1	N.A.	-6	-5
5A	**UV-VIS hyperspectral imager with dispersive elements on orbiter**	SS	UV-Vis	512x512	1	4	4	N.A.	N.A.	+2	-2	-1	-1/0	-1/0	+1	-	-2
6Au	**TIR Hyperspectral/Multispectral imager on rover**	PE	TIR	512x256	1	4	4	+1	-2	+2	-2	-2	-1	-2	0	-7	-6
6Ac	**TIR Hyperspectral/Multispectral imager on rover**	PE	TIR	512x256	1	4	4	+2	+1	+2	+2	-2	-1	-2		-1	0
7Au	TIR Hyperspectral/Multispectral imager on orbiter	PE	TIR	160x120	3	4	4	0	-2	+2	-2	-2	-1	-2	0	-10	-8
7Ac	TIR Hyperspectral/Multispectral imager on orbiter	PE	TIR	160x120	3	4	4	+1	+1	+2	+2	-2	-1	-2	+2	-4	-2
8A	TIR Multispectral imager on nano/micro/minisatellite	EO	TIR	128x16	3	4	4	N.A.	N.A.	+2	+2	-2	-1	-1/-2	+2	-	-1.5

Legend:c= cooled; u = uncooled. N.A. = Not Available.

Table 3 – Novel CS-based instruments (novel CS approach).

Conf. #	Short description	Field	Spectral range	Number of pixels	Integration time (1→3)	TRL HW	TRL SW	Mass reduction % (-2→ +2)	Power reduction % (-2→ +2)	Partial mass red. % (-2→ +2)	Partial power red. % (-2→ +2)	Comp. burden (-2→ +2)	Compression ratio (-2→ +2)	Info content accuracy (-2→ +2)	Cost reduction (-2→+2)	Final ranking
1B	**Punctual / whiskbroom spectrometer on rover for detecting the presence of pre-selected substances**	PE	VIS - SWIR	512 x 1 (Data output)	1	4	3			+2	+2	+1/+2	+1/+2	-1/0	+2	**8**
2B	Punctual / whiskbroom spectrometer on orbiter for detecting the presence of pre-selected substances	PE	UV-NIR	512 x 1(Data output)	1	4	3			+2	0	+1/+2	+1/+2	-1/0	+2	**6**
3B	**Camera operating in the MIR-TIR for sky observation and real-time detection of Near Earth Objects (NEO)**	SS	MIR-TIR	512x512	1	4	3			+2	+2	+1/+2	+1/+2	-1/0	+2	**8**
4B	Star-Tracker, with dual use for asteroids detection	SS	VIS	512x512	2	4	3			-2	0	+1/+2	+1/+2	N.A.	-1	**-2**
5B	**Pushbroom imager for thematic maps generation**	EO	VIS - NIR	512 x 1 (Data output)	2	4	3			+2	+2	+1/+2	+1/+2	-1/0	+1	**6**
6B	THz single-pixel imaging with a Si wafer based optical modulator and IR single-pixel imaging with a DMD based modulator	SS	THz, IR	32x32	2	3	4	0	0			-1	-1	-1	0	**-4(#)**
7B	CS based atmospheric sounder for sub-millimeter wave band	EO	THz	140	1	3	4	0	0			-1	0	-1	0	**-2(#)**

(#) For the two concepts in the THz range, we considered total mass instead of partial mass for final ranking since partial mass was not available.

In order to investigate the full potential of CS technologies in space applications, one configuration out of the classical CS concepts and one configuration out of the novel ones were selected for the preliminary design.

The selected configurations were:

- Concept #5A – "UV-VIS hyperspectral imager with dispersive elements on orbiter", which relies on a classical CS approach addressing the reconstruction of the full image/signal.

- Concept #3B - "Camera operating in the MIR for sky observation and real-time detection of Near Earth Objects (NEO)", which relies on a novel CS approach aiming at information extraction without prior full reconstruction of the image/signal. Concept #3B was regarded as particularly

interesting since NEOs detection is definitely a 'hot topic' at international level and ESA is also planning specific missions on this subject.

The subsequent phase of the project consisted in the preliminary design of these two configurations. The preliminary design of both instruments showed some advantages in terms of mass and power consumption budgets, although to a limited extent. However, differently from instrument #5A, the preliminary design of instrument #3B raised some critical implementation aspects. In particular, some HW components were not commercially available: the lack of a suitable single element detector poses a serious drawback, which made the choice of this instrument very risky for the continuation of the project. On the other hand, instrument #5A followed a more conservative approach and the technologies needed for its construction were all commercially available. As a consequence, instrument #5A was selected for the Detailed Design phase of the project. Considered the limited extent of the advantages in terms of HW budgets with respect to a traditional system, the proposed configuration was further analysed to explore the possibility of improving its performance and/or extending its field of application. In the following section we summarize the preliminary design of instrument #3B and the detailed design of instrument #5A.

4 PRELIMINARY DESIGN OF CONCEPT #3B

The proposed instrument was inspired by the NEOWISE project funded by NASA's Planetary Science Division that detects the presence of asteroids and comets from images collected by the Wide-field Infrared Survey Explorer (WISE) spacecraft. The proposed concept aims at combining a sky survey with image acquisition to the on-board detection of NEO, instead of data-mining and processing of the acquired images at ground.

The proposed concept is a single-pixel CS-based panchromatic camera working at 3-5 μm. This circumstance entails a payload cooled down to about 150 °K. The use of a DMD as SLM was initially investigated. The main drawback was the minimum working temperature declared by the producer for this type of devices (233 °K). For this reason, the use of a DMD as a SLM seemed very difficult since the signal-to-background ratio that could be achieved at 233 °K was far from being acceptable. The proposed payload architecture overcomes this problem by suggesting the use of a coding mask instead of the DMD. The mask could be obtained through photolithographic deposition of a pre-defined, ad-hoc, CS modulation pattern on a glass support transparent in the MIR. In this case, the change in modulation was obtained by using an X-Y linear stage and the modulation speed is limited by the speed performance of the linear stage.

The proposed payload consist of the following main elements: a telescope, a coding mask with an X-Y movement stage, a condenser lens, a single element detector, a proximity electronic board, temperature controller and coolers. Finally, a processing unit (PDHU) and power supply were foreseen. An outline of the payload is shown in Fig. 1a, while the layout of the optical design is reported in Fig. 1b. The telescope is the entrance optics of the payload. Its characteristics are similar to the input optics of WISE mission. The telescope has a focal length of 1871 mm, a diameter of 500 mm and a field of view of 0.784 deg. It produces a panchromatic image of the observed portion of sky on a coding mask placed in the image plane of the telescope. The mask is obtained through the photolithographic deposition of a modulation pattern on a glass support transparent in the MIR. The physical dimensions and the total number of pixels of the coding mask depend on: the pixel pitch, the desired final image pixel number and the number of modulations needed for the reconstruction. For this concept, the pixel pitch was set to 50 μm; the image pixels to 512x512 and the required different modulations to (512*512)/10, corresponding to p=0.1.

A linear X-Y stage moves the coded mask so that after each movement a different CS pattern is placed in the image plane. The stage must be able to perform a single step movement of 50 μm in 0.2 ms (linear speed of 250 mm/sec); after each movement, the stage must stop for 0.8 ms during which the signal is acquired. The travel range of the stage is given by the actual part of the mask

that is moved. In this configuration the travel range is 8.1 mm x 8.1 mm. The mask size and the stage travel range can be reduced by limiting the number of available modulations.

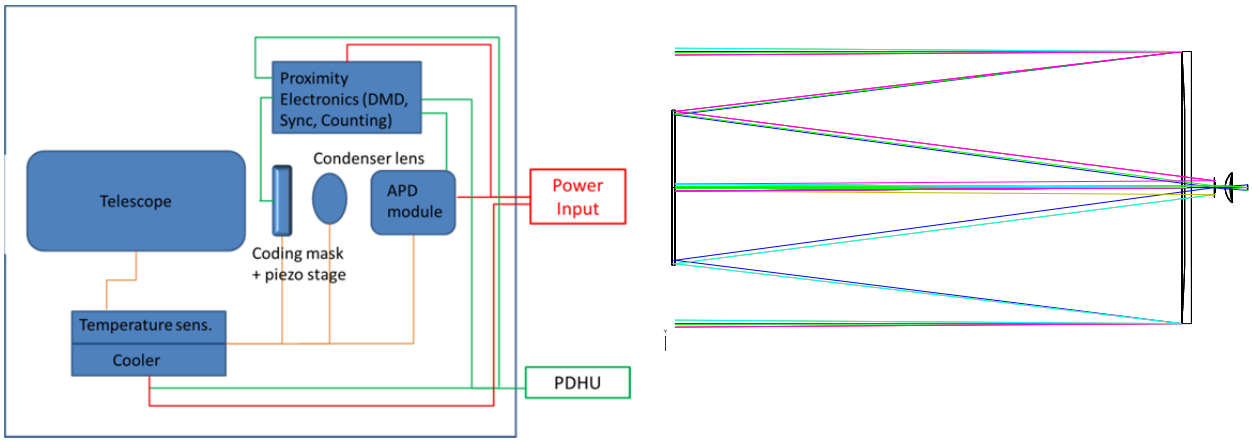

(a) (b)

Fig. 1 – Concept #3B: a) Schematic diagram; and b) Layout of the optical design for #3B payload.

A condenser lens concentrates the image, CS-coded by the mask, on a single-element sensor. The sensor is a Mercury Cadmium Telluride (MCT) APD working in photon counting mode, since few photons (photoelectrons) are expected to impinge on the detector during each CS measurement. The expected flux of radiation impinging on the coding mask and detected by the APD during each measurement was numerically simulated considering a realistic scenario. The optical system has a fully planar, in-line design and works totally in transmission. The spatial resolution is limited only by the large Airy disk size. The beam is projected unfocused on the single element sensor and the sensor is placed at the beam minimum diameter.

The proximity electronics supervises the stage movement, counts the pulses coming from the APD and synchronises the movement of the stage with the counting operation. The payload should work at low temperature (about 150 °K), except for the X-Y movement actuators that cannot work at temperature below -40°C. Temperature control, heaters and coolers should be foreseen.

The proposed preliminary configuration shows several critical HW-related issues. In particular, two components are critical: the MCT APD detector working in photon counting mode with a large sensitive area and the piezoelectric stage and drive electronics that should have high speed for single step movement. Both are not available as COTS components. Presently, there are not simple solutions to these critical issues, except for analysing and reaching a trade-off on the payload performance. For example, an increase in integration time, which needs a more stable platform, would decrease the requirements for the speed of the piezo-stage and would also increase the signal intensity, thus suggesting the possibility to use standard MCT or PbSE sensors.

4.1 Preliminary payload budgets assessment

The expected mass and volume reduction with respect to the traditional instruments is quite limited (about 1–kg mass reduction); thus, the major advantage of the CS approach is expected in terms of data transmission requirements.

The overall mass estimate for the optical head plus the front-end electronics (FEE) and the internal calibration unit (ICU) is 25 kg, including a contingency of 20% (20 Kg for the optical head and 5 Kg for FEE+ICU). A comparison between the budgets expected for the main components of the CS-based system and those of a corresponding traditional system is given in Table 4.

Table 4 - Concept #3B: Budgets for the CS-based system and for the traditional counterpart.

CS-based system		
Component	**Weight**	**Power**
Coding mask	20.7 gr	not available
Movement stage	TBD	TBD
Condenser (ZnSe)	65.2 gr	not available
MIR Single element detector	TBD	TBD
Traditional system		
Component	**Weight**	**Power**
MCT Sofradir Uranus 640x512	700 gr	10 W; 25 W (cooled down)
Compression board	1000 gr	20 W

4.2 Preliminary performance analysis

Images coming from the WISE database were used as input for image simulation of instrument #3B. Starting from the WISE images converted in photons, a region of 512x512 pixel was extracted and "synthetic" NEOs added to it. The NEOs were simulated as spherical objects of given temperature, by using their Black Body spectral radiation curve.

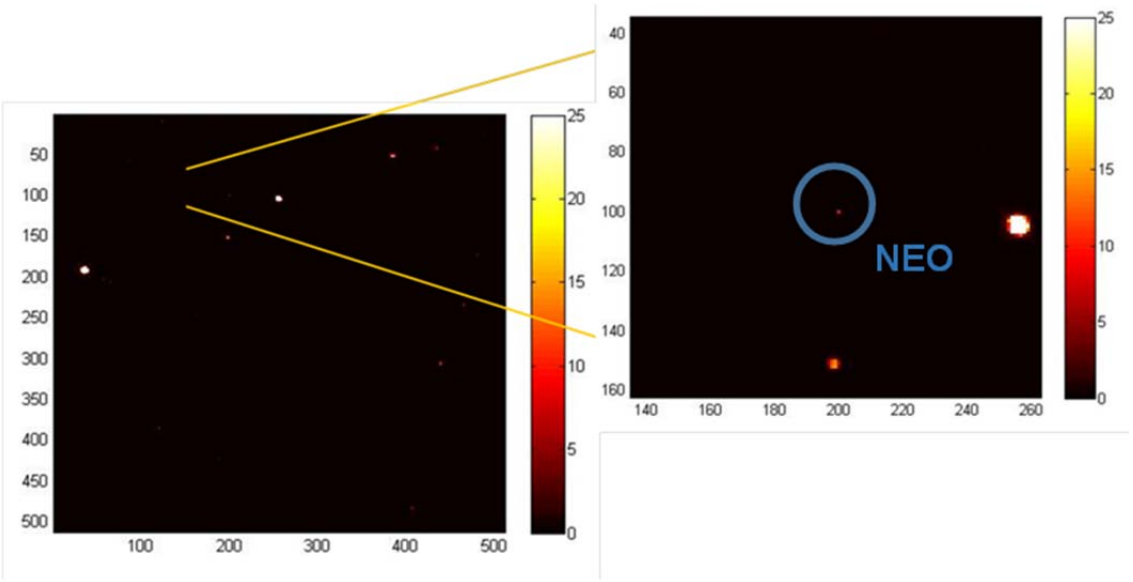

Fig. 2 – Concept #3B: Simulated image in photon/pixel and detail of the region containing a NEO.

The acquisition with instrument #3B does not follow the ideal linear model typical of CS, because the acquired measurements are affected by photon noise and by the emissivity of the DMD. As stated above, the system performance was significantly limited by the DMD emissivity. This in practice meant that, even if the detection of a NEO was possible, the emissivity degraded the quality of the reconstruction of the background to an unacceptable level when the DMD worked at the lowest temperature allowed by the constructor. On the other hand, the use of a mechanical moving mask posed additional constraints on the design of the sensing matrix, namely: *i)* to correspond to a mechanically shiftable pattern, and *ii)* to have the distance-preserving characteristics necessary for CS reconstruction. For this purpose, a matrix having both characteristics, namely, a block circulant with circulant blocks (BCCB) matrix, drawn from a symmetric Bernoulli distribution, was designed. In addition, the selected matrix permitted fast decoding using the bidimensional FFT.

We tested the reconstruction performance of both NEOs and background, with a compression ratio of 10:1, the results in Fig. 3 report the reconstructed image ordered row-wise, where pixel values are represented as circles. As expected, despite the presence of noise, there are not major

problems to detect NEOs and recover the background, when the NEO is intense enough (Fig. 3 - Reconstruction examples for instrument #3B with compression ratio 10. a)Intense NEOs. b)Weak NEO.Fig. 3a). On the other hand, when NEOs have a weaker intensity, we are able to recover the most intense NEOs by tuning the sparsity of the sensing matrix. Although a NEO with intensity comparable to the level of photon noise can be still recovered, we are not able to distinguish it from the rest of the image without having any side information about its position (Fig. 3b). On the basis of these results, the detection limit was set to 10 photons (equivalent to approximately 20 photons at the telescope entrance), corresponding for example to NEOs with the characteristics listed in Table 5.

Table 5 - NEOs detection limits with the system cooled at 150 °K.

Distance	NEO minimum diameter	NEO temperature
0.5 AU	21 km	300 °K
0.5 AU	3.5 km	400 °K
1 AU	15.5 km	350 °K
1 AU	7 km	400 °K

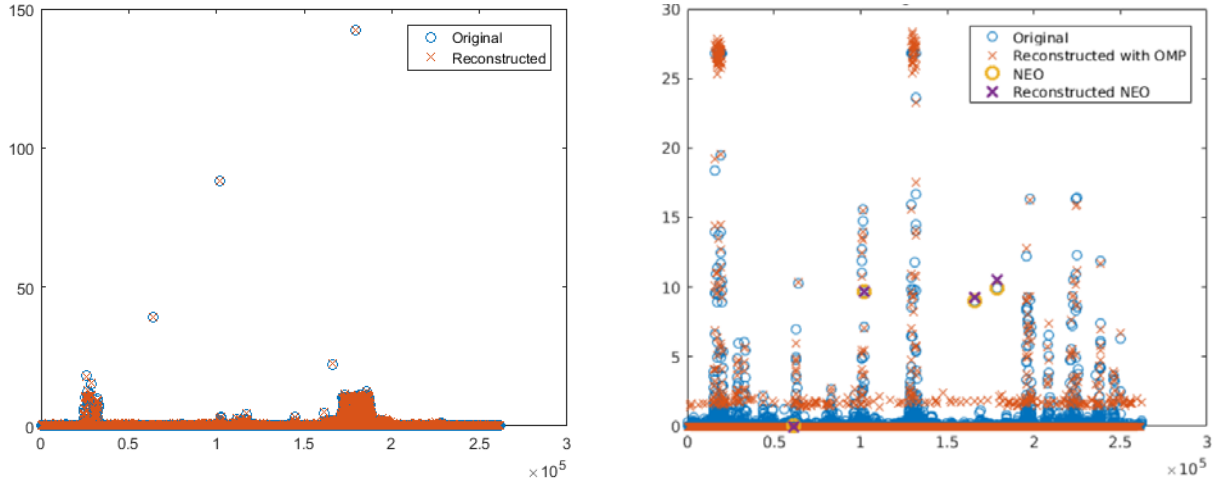

(a) (b)

Fig. 3 - Reconstruction examples for instrument #3B with compression ratio 10. a)Intense NEOs. b)Weak NEO.

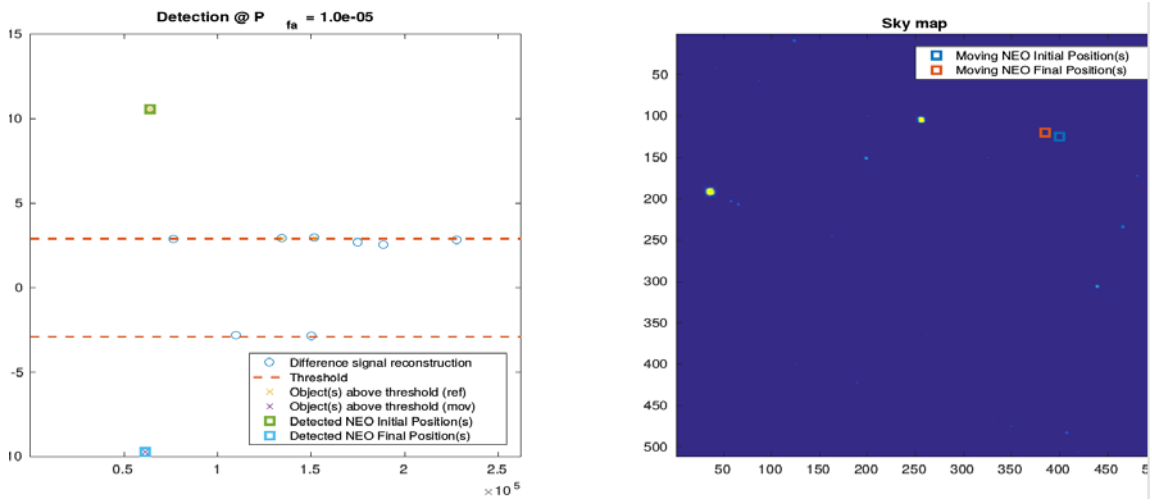

(a) (b)

Fig. 4 – a) Identification of outliers; and b) Sky map with moving NEO detected.

We also showed the feasibility of a moving NEO detection scheme working directly from the measurements of subsequent frames. The activity required the design of an ad-hoc algorithm, which

allows tuning the detection performance using the Probability of False Alarm as a parameter. The following figures (Fig. 4a and b) show that even with a relatively high False Alarm of 10^{-5}, the algorithm is robust and able to detect the NEOs among the outliers.

5 DETAILED DESIGN OF CONCEPT #5A

The proposed CS-based instrument was conceived as an imaging spectrometer/photometer - working in the UV–VIS - implemented for slitless spectroscopic/photometric astronomy and operating from geostationary or sun-synchronous platform with total measurement time similar to the ones of the STIS on Hubble Space Telescope (HST). Such CS instrument, reducing the detector throughput, requires a lower memory capacity and narrower down-link bandwidth. The choice was also motivated from a partial lack of such instrument among the operative SS satellites. Presently, there are only two instruments working in the UV - VIS: the STIS instrument on board of the Hubble Space Telescope and the Blue Photometer on board of GAIA mission. The payload is made up of the following main elements: a telescope, an imaging spectrometer, a DMD as SLM, a condenser lens, a single element detector, a proximity electronic board, a temperature controller and heaters. A data handling/processing unit (PDHU) and power supply must be also foreseen. The outline of the payload architecture is shown in Fig. 5a. This was designed using COTS components. The optical design was performed by considering a modular structure for the different optical components.

The telescope is the entrance optics of the CS payload. The telescope has focal length of 2321 mm, a diameter of 235 mm and a field of view of 0.273 deg (IFOV 5.33E-04 deg). The telescope is a Schmidt-Cassegrain designed with a parabolic surface for the primary mirror and hyperbolic surface for the secondary mirror. The selected material was coated aluminium since it has an improved transmittance in the UV - VIS spectral range and is compatible with space environment. The folding mirror M1 feeds the image produced by the telescope to the input of the imaging spectrometer. The spectrometer is a prism-based one, designed for performing slitless measurements. The spectrometer block depicted in Fig. 5b is composed by a collimating optics, a prism and an imaging optics. The instrument was designed to be pixel-limited in the entire 300 nm - 650 nm spectral range. The spectral sampling ranges from 2.2 nm @ 300 nm to 22 nm @ 650 nm, with a total of 50 samples for each spectrum. The spectral sampling is similar to the one of the GAIA mission. The system straylight was analysed and the results were exploited to design an adequate system made of several baffles (Fig. 7) to mitigate straylight effects on the acquired signal. The main purpose of the folding mirrors is to make the instrument more compact. After the second folding mirror, the signal is fed to the spectrometer to produce a hyperspectral image of the observed section of the sky, focused on the DMD after a third folding mirror. The DMD performs the CS coding by spatially modulating the incoming light. The selected DMD chip is one of those produced by Texas Instrument, designed for operation in the UV, with an array dimension of 1920 × 1080 aluminium mirrors having a pitch of 10.8 μm. The DMD window transmittance is greater than 85% in the considered spectral range. The DMD reflects the coded image to a condenser lens. The condenser lens concentrates the image on a single element detector (Fig. 6b), thus performing a spatial integration of the CS coded image. The single pixel sensor is a PMT module. The latter works in photon counting mode due to the small amount of photons (photoelectrons) that reach the sensor during each CS measurements. The expected flux of radiation reaching DMD and PMT during each measurements was numerically simulated considering a realistic scenario.

The proximity electronics supervises DMD coding operation, counts the pulses coming from PMT module, and synchronises the generation of the CS masks on DMD with counting operation. The electronics should be kept close to DMD to minimise the length of the flex cables. Temperature control and heaters should be also implemented.

The optical system has a non-planar design due to the fact that the DMD micro-mirrors rotate

along a diagonal axis. This adds to the reflected direction a 45° rotation out of the plane formed by the telescope and spectrometer optical axes.

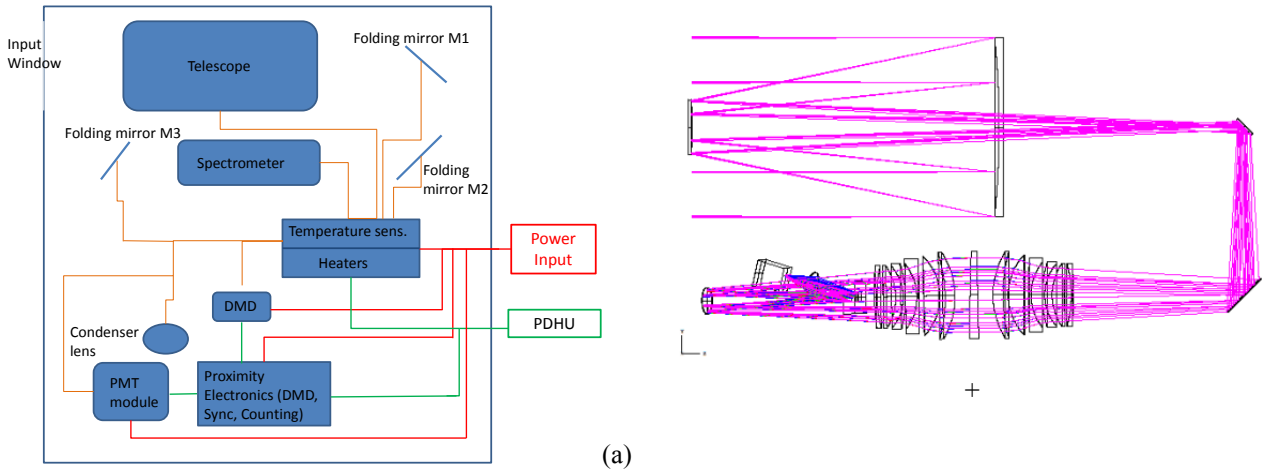

Fig. 5 - Concept #5A: a) Schematic diagram for the payload; b) Layout of the optical design.

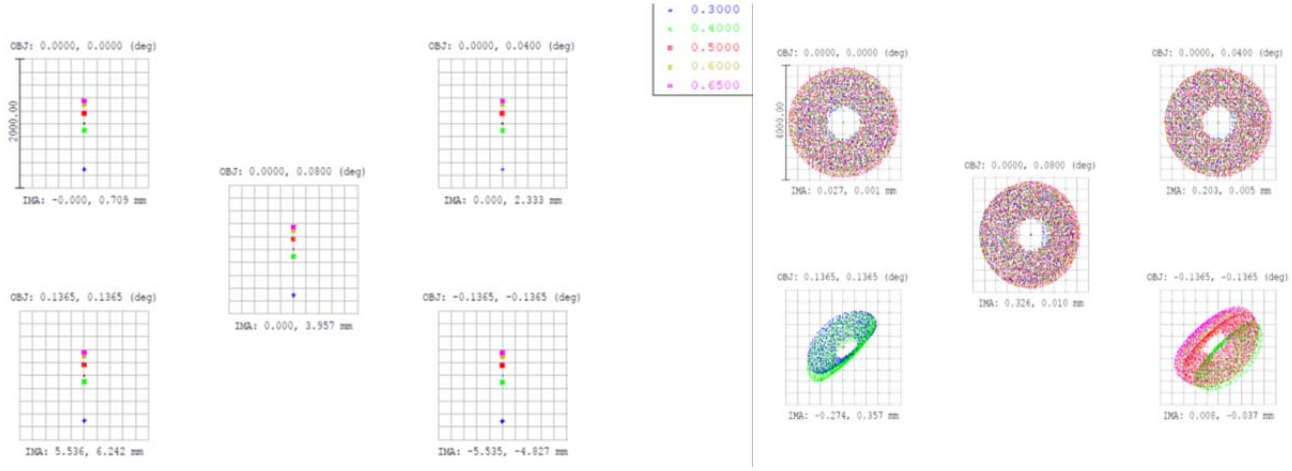

Fig. 6 - Concept #5A: a) spectrum on the image plane (DMD surface) for different angles in the instrument field of view; and b) Spot radius on the PMT.

In order to reduce the effects of stray light on the acquired signal, a system made of several baffles was designed (see Fig. 7).

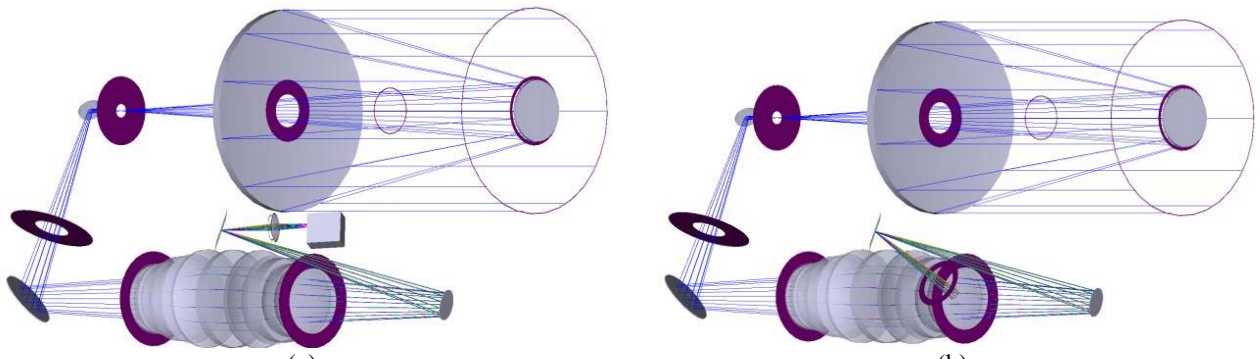

Fig. 7 - Concept #5A: Zemax 3D instrument layout with baffle system: a) DMD with mirrors in the on position; and b) DMD with mirrors in the off position.

Since CS instruments rely on the acquisition of only a fraction of the received signal, stray

light mitigation is particularly important. In the case of Instrument #5A, stray light mitigation is even more crucial since the signal received from stars is expected to be weak and the scene is highly sparse. The designed baffles perform straylight suppression along the entire instrument path. In particular, this ensures the protection from internal reflection of the condenser and the detector and the trapping of the light reflected by the micromirrors in OFF position.

5.1 Payload budgets assessment

The overall budget assessment for the mechanical arrangement is the following:

Dimensions estimate:

- Optical Head (OH): 870 mm x 642mm x 507 mm
- Front End Electronics (FEE): 200 mm x 140 mm x 80 mm;
- Main Electronics (ME): 240 mm x 200 mm x 80 mm

Mass estimate:

- Optical Head: 25.4 kg (including contingency 20%) (see Table 6)

FEE + ME: 5 kg (including contingency 20%)

Power estimate:

- < 30 W (assumptions: DC/DC Efficiency = 9.75 ; contingency 20%)

Table 6 – Concept #5A: Detail for Optical Head mass estimation.

Component	***Mass (Kg)***
Optical bench	8
Optics	4.7
Spectrometer support	1.6
Folding support	0.8
Bipods	1.5
Telescope	1.5
DMD-PMT-Trap group	0.8
MLI (Multi-Layer Insulation)	1.5
Harness & screw	0.8
Total mass (without contingency)	21.2
Contingency 20%	4.2
Total Mass with contingency	25.4

The comparison of the budgets of the CS-based system main components with those of the traditional one is reported in Table 7.

Table 7 – Concept #5A: Comparison of the budgets for the CS-based system components and those of the traditional one.

Standard CS-based system		
Component	**Weight**	**Power**
DMD	10 gr (estimated)	4.4 W (chip)
Condenser (fused silica)	9.69 gr	not available
PMT	47 gr	0.24 W
Traditional system		
Component	**Weight**	**Power**
CCD	8 gr	0.014 W
Compression board	1000 gr	20 W

In summary, the main advantage of the CS-based instrument is the elimination of the data compression board. This offers an advantage in terms of power consumption, so that the power

absorbed by the CS instrument decreases (about 15 W) with respect to a traditional one, and in terms of mass, although to a limited extent (about a 1-kg decrease). The lack of a compression board also avoids the need of implementing an *ad-hoc* compression algorithm, along with the development costs of an electronic board. The volume of the instrument does not show a significant decrease: despite the possibility of replacing a matrix detector with a single element detector, the optical components that have the major impact on the instrument's volume, such as the entrance optics and the spectrometer, have the same size as in the corresponding traditional instrument.

5.2 Data simulations and performance analysis

A number of simulated images were produced and used as input to the reconstruction algorithm. On the whole, we generated 4 sets of simulated images:

1. Reference images, without system MTF, noise and detector sensitivity (ideal images).
2. Images with system characteristics taken from the preliminary design.
3. Images with Gaussian MTF, in order to test the reconstruction algorithm with MTF compensation, by using MTF with a simple shape and non-wavelength-dependent.
4. Images with the system characteristics taken from the detailed design, including spatial-spectral dependent MTFs.

These four set of images shared the simulation procedure and some input data:

- Spectrum of stars coming from STIS spectral library.
- Sky background flux (accounting for Earthshine and Zodiacal Light) as evaluated for STIS.

Instead, other inputs were changed during the project following the evolution of the system design.

In Fig. 8 a simulated image (set n.4) is reported together with a detail of the region containing stars spectra. The smoothing caused by PSF is clearly visible, although limited thanks to the optimization performed on the optical system design.

From the point of view of data reconstruction quality, the results showed a good performance of the designed instrument. Quality assessment of reconstructed data was performed by measuring several quality metrics, chosen among those recommended by CCSDS, and by comparison with the outcomes of CCSDS-IDC data compressor.

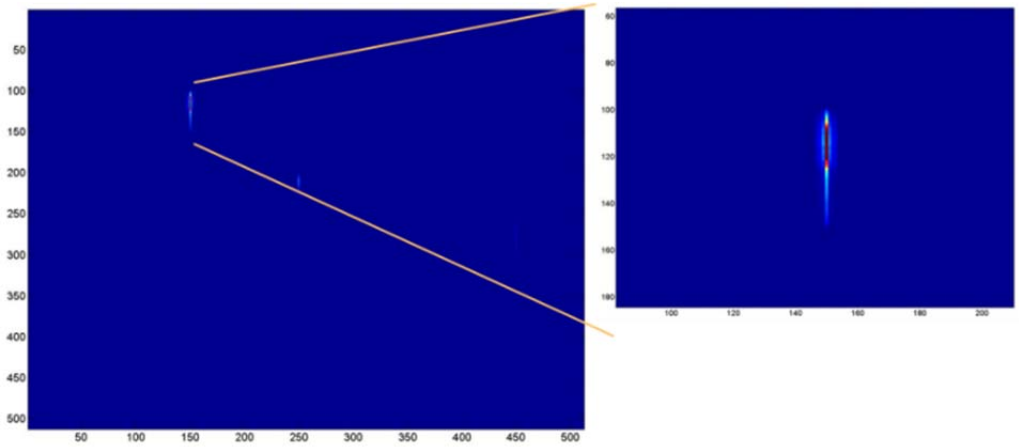

Fig. 8 - Concept #5A: Simulated final image in counts, with a detail of the spectrum obtained for HD140232.

All the tested metrics showed a consistent behaviour, where a lower CR corresponds to higher quality. In terms of rate-distortion trade-off, the results obtained showed that the R-D performance of the CS-based instrument is satisfactory, as at high compression ratios the CS-instrument outperforms a conventional instrument equipped with a standard data compression board, whereas the performance loss of the CS-instrument is limited at medium compression ratios. However, the images are affected by a relevant amount of noise, which limits the achievable quality of the CS-

based instrument. Anyway, it should be noted that this significant amount of noise would affect as well the performance of a conventional instrument. In the high compression ratio regime, these results are expected to translate into a downlink gain with respect to a standard tool, even if equipped with a compression board. Actually, the designed instrument can achieve compression ratios of 20 and even higher without a significant loss of data quality. Our aim is to recover the image compensating the effects of MTF and noise, neglecting other effects such as the Quantum Efficiency or the transmittance. Without any knowledge of the star positions, we can integrate in the reconstruction algorithm the compensation of the MTF affecting the image background, comparing it with an *a posteriori* compensation of the MTF after the image reconstruction (Fig. 9 a and b).

We also show that having a side-information available about the position of the star spectra in the image significantly improves the reconstruction quality, as it allows compensating the MTF affecting the significant image components, *i.e.*, the star spectra, as can be noticed in the following figures (Fig. 10 a and b). This additional side-information can be obtained using an instrument with 2 arms, as described in the following section.

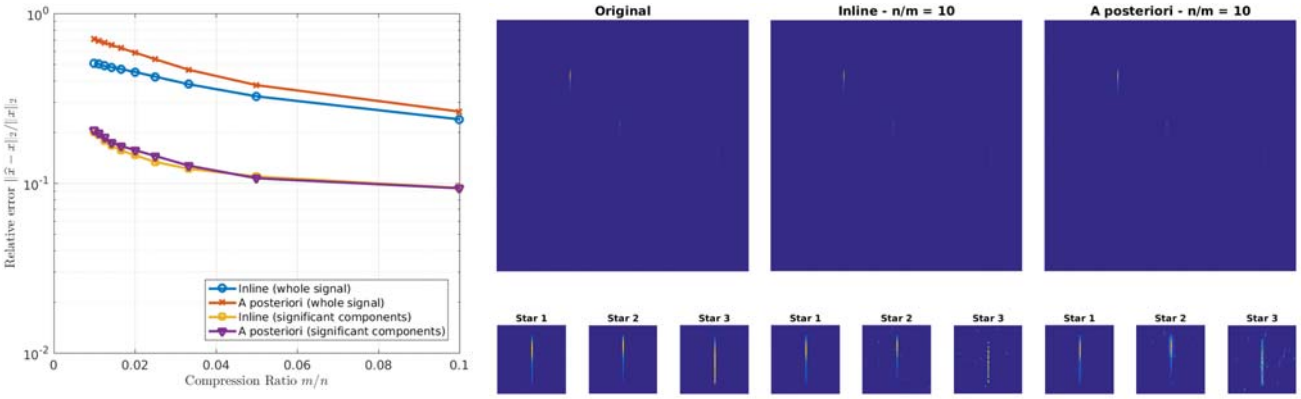

(a) (b)

Fig. 9 – MTF compensation: a)Relative error as a function of relative number of measurements; and b)Reconstruction for n/m = 10.

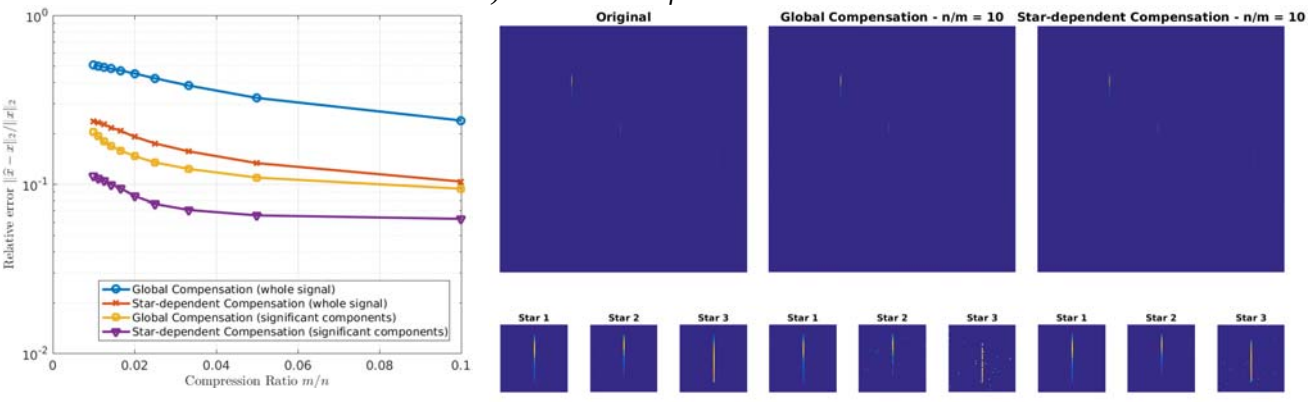

(a) (b)

Fig. 10 – MTF compensation with star position: a) Relative error as a function of relative number of measurements; and b) Reconstruction for n/m = 10.

5.3 Preliminary Design of a double arm configuration of concept #5A

In configuration #5A, the light reflected by the DMD mirrors in the off position is dumped. An additional issue that was explored in the course of the project was the feasibility of exploiting this radiation – usually dumped - in order to implement an additional channel or functionality of the system. Two types of functionality could be identified:

1) Exploiting the 'usually-dumped' light to obtain a better signal quality,
2) Exploiting the 'usually-dumped' light to implement an additional channel and obtain further

information on the scene under observation.

Both solutions imply the construction of a double-arm configuration: the first arm implements the channel of the single-arm instrument #5A described so far, the second arm implements the additional channel used for improving the system performances, either in terms of signal quality or additional applications.

If the first solution is adopted, the double-arm architecture will be able to acquire both the modulated scene and its dual one. This solution uses the 'rejected' light to improve the SNR of the reconstructed data. On one hand, this solution offers the opportunity to increase the integration time thanks to the parallel acquisition, yielding a better quality of the reconstructed images. On the other hand, it requires an additional condenser and detector, decreasing the budget gain with respect to a traditional instrument.

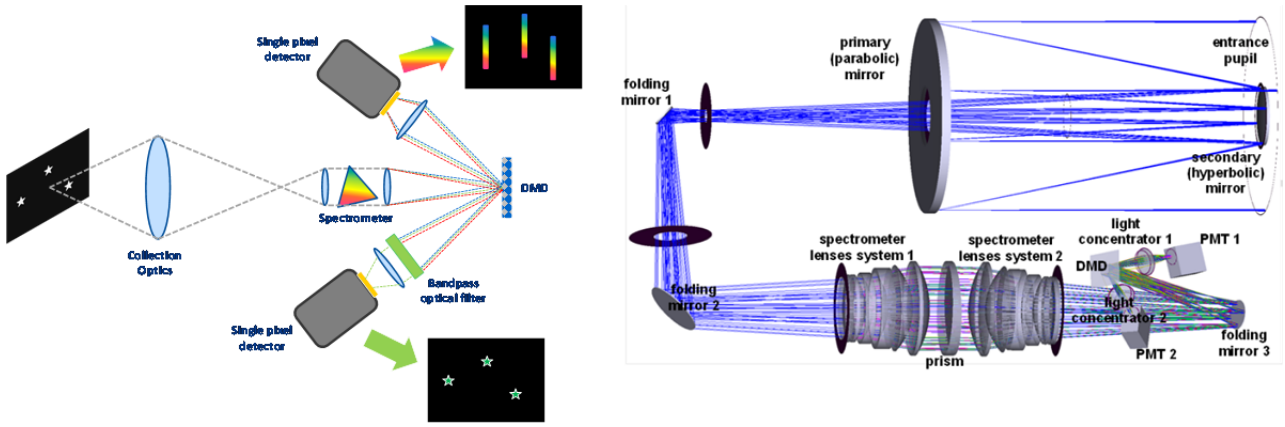

Fig. 11 – Concept #5A – double arm configuration: a) architecture with two CS-arms, one for slitless spectroscopy and the other for stars position determination; and b) preliminary optical design.

If the second solution is adopted, the first channel can be used to perform slitless spectroscopy, while the second channel could be used to determine the stars position by adding a narrow band-pass filter. This information could be effectively used as an input to the reconstruction algorithm to improve the SNR of the reconstructed data.

Since the image on the second channel would be highly sparse, it is likely that it can be reconstructed using a small number of measurements. In addition, if the star position can be reconstructed on board, this information could be further useful in two ways: (1) for the construction of Regions Of Interest (ROIs) on the DMD in order to acquire only the areas of interest, yielding an increased accuracy with respect to defining the ROIs on the basis of star catalogues; (2) for obtaining additional information, such as the detection of non-stellar objects (NEO, debris), by comparing the detected stars position with that from stars catalogues.

To sum up, the latter solution provides additional information on star position to be used as input to the reconstruction algorithm to improve the SNR of the reconstructed data and to increase the accuracy on this piece of information with respect to a catalogue-based star position. On the other hand, this solution requires an additional condenser and detector - plus a bandpass filter, thus decreasing the budget gain with respect to a traditional instrument. Taking into account the pros and cons of both solutions, the second solution aiming at the implementation of an additional functionality of the instrument was regarded as very interesting. Thus, a preliminary design of a double-arm configuration implementing this functionality was carried out.

Table 8 – Concept #5A – Comparison of preliminary budgets for double arm and single arm configurations.

Single arm CS-based system		
Component	**Weight**	**Power**
DMD	10 gr (estimated)	4.4 W (chip)
Condenser (fused silica)	9.69 gr	not available
PMT	47 gr	0.24 W
Double-arm CS-based system		
Component	**Weight**	**Power**
DMD	10 gr (estimated)	4.4 W (chip)
2 Condenser (fused silica)	19.38 gr	not available
Bandpass optical filter	5 gr (estimated)	not available
2 PMT	94 gr	0.48 W
Traditional system		
Component	**Weight**	**Power**
CCD	8 gr	0.014 W
Compression board	1000 gr	20 W

The architecture of this double-arm configuration is depicted in Fig. 11, together with its preliminary optical design. The instrument is basically the same described in the previous sections, except for the introduction of a second arm constituted by a condenser lens, a narrow-band spectral filter and a single pixel detector. For this reason, the dimensions estimate does not change with respect to the single arm configuration. As for mass and power estimates, there is only a small increase: the total mass is 32.7 kg (including contingency 20%) and power estimate is 30.3 W.

Table 8 compares the preliminary budgets of both the double-arm and the single-arm configurations with those of a corresponding traditional system.

5.3.1 Data simulations and preliminary performance analysis

Data simulation was also performed for the implemented second arm (channel 2). These simulations were useful to assess if - and to what extent - the availability of information on stars position impacted on the reconstruction algorithm and the data reconstruction based on the data from the first arm (channel 1). The information coming from channel 2, in principle, can be used also for the detection of NEOs. Thus, a preliminary assessment of the limit for NEO detection and a first analysis for Space Debris detection were also performed. The minimum detectable NEO dimensions were evaluated for NEO with albedo equal to 0.03, 0.1 and 0.5. If we define the minimum detectable signal as 20 counts, we can estimate the minimum detectable NEO dimensions as a function of NEO distance from the Earth and NEO albedo (Table 9).

Table 9 – Concept #5A – Double arm configuration: NEO Detection Limit.

Distance from NEO/Albedo	**Minimum detectable dimensions (Detection limit = 20 counts)**
0.5 A.U /. Albedo 0.03	2 Km
1.0 A.U /. Albedo 0.03	4 Km
1..5 A.U /. Albedo 0.03	10 Km
0.5 A.U /. Albedo 0.1	1.5 Km
1.0 A.U /. Albedo 0.1	2.5 Km
1..5 A.U /. Albedo 0.1	6 Km
0.5 A.U /. Albedo 0.5	0.5 Km
1.0 A.U /. Albedo 0.5	1 Km
1..5 A.U /. Albedo 0.5	2.5 Km

From the point of view of the reconstruction algorithms, we successfully tested the possibility

of compensating the instrumental response of the sensor together with the reconstruction of the data. This represents a considerable advantage, since it permits skipping a step that is typically required for processing data from spectroscopic observations of the sky. The MTF compensation also yielded to a slight improvement (a few percent, at least) in the quality of the reconstructed data (at the same CR).

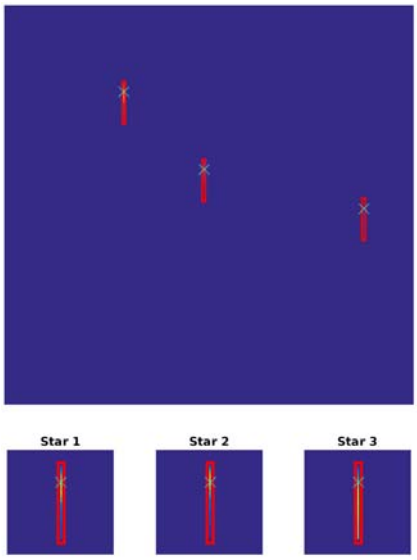

Fig. 12 – Position of stars on channel 2 and spectra on channel 1 of the double-arm configuration.

The aim of the activity is to improve and simplify the reconstruction of the image on channel 1 by exploiting as side information the estimated star positions obtained reconstructing the image on channel 2, since there exists a prescribed relation between the position of the stars on channel 2 and the position of the star spectra on channel 1 (Fig. 12).

The following figures (Fig. 13a and b) show that a significant improvement can be obtained with the double-arm configuration, which can be noticed by comparing the curves labelled with *Pinv*, describing the performance of this novel configuration, with the curves labelled with *OMP*, depicting the performance of the standard configuration.

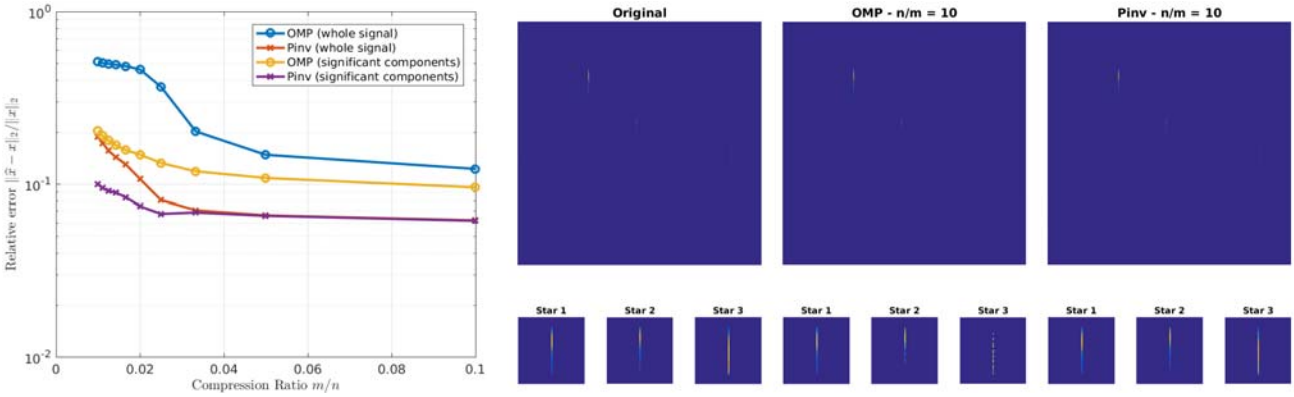

(a) (b)

Fig. 13 – Double-arm configuration: a) Relative error as a function of relative number of measurements; and b) Reconstruction for n/m = 10.

The results of the preliminary design of this additional '*two-in-one*' instrument – that was not initially foreseen in the project's activities – were particularly promising. The instrument is more flexible and shows increased performance. First of all, the information from channel 2 can be used

as input for the reconstruction of the data from channel 1, permitting the use of faster and more accurate algorithms and thus opening also the possibility of on-board data processing. The information coming from the second arm can be used not only as side information, but it can be exploited for new applications, such as NEO detection. Moreover, *ad hoc* algorithms, individually tailored for the reconstruction of two data-sets, can exploit several novel prospects related to different operational modes, such as synchronous/asynchronous acquisitions, adaptive ROI definition, etc.. By extending the concept, is possible to think to a unique instrument that implements two different applications. Moreover, different operational modes could also improve instrument performance in terms of computational burden and downlink budget.

5.4 Market Analysis and Qualification Status

The technological development of the two key CS components, the SLM and the detector, has not yet achieved such a maturity level to express the full potential of CS in space applications.

As far as the SLM is concerned, the state-of-the-art technology permits to actuate micromirrors changing their orientation and its vertical position in the direction orthogonal to the average mirror surface. The main producer of the DMDs currently available on the market is Texas Instruments, but also few Research Institutes have obtained important technology outcomes on DMD fabrications. The latter devices work only in reflection and only a limited range of dimensions is available for the micromirrors. Their space qualification is still on going, but several studies have been performed in last years. Tests performed for Euclid ESA mission put in evidence that the DMD remains fully operational at -40°C and in vacuum, but some micromirrors failures were found when the selected DMD experienced temperature below -40°C. Test results did not reveal any concerns regarding the ability of the DMD to meet environmental space requirements (Zamkotsian et al. Successful evaluation for space applications of the 2048x1080 DMD, Proc. of SPIE Vol. 7932, 79320A). Recently, Rochester Institute of Technology together with NASA and Johns Hopkins University has performed a complete and detailed study for space qualification of the TI DLP7000 device (Travinsky et al. in the paper "Evaluation of Digital Micromirror Devices for use in space-based Multi-Object Spectrometer (MOS) application" submitted to J. of Astronomical Telescopes, Instruments, and Systems, 2017). The extensive work summarizes the results of a continuous investigation on the performance of DMDs under conditions associated with space environment. The response of DMDs to radiation, to vibration and mechanical shock associated with launch, and the behaviour of DMD under cryogenic temperatures were tested. The study demonstrates that DMDs operate smoothly at temperatures at least as low as 78°K and that they are extremely robust, so that they can be considered as a reliable alternative to micro shutter arrays (MSA) in space applications. On the other hand, other SLM types like LCOS or MSA are not suitable for this specific application: the former cannot be space qualified and the latter are too slow and with few elements. Since the interest in the development of this type of devices is increasingly high, a substantial technological development is anyway expected in this field in the next years.

As far as the detector is concerned, their development strongly depends on manufacturers, but recommendations can be done in order to produce more performant detectors for CS applications in space. Given the very weak light intensity to be measured, the detector usually works in photon counting mode. It must have high quantum efficiency, a large sensing area and very low dark count rate. On these lines, the PMTs would need better quantum efficiency. The bialkaly photocathode, that was our choice for the detailed design, has a peak quantum efficiency of 43% at 350 nm. Beyond this wavelength, the quantum efficiency decreases rather rapidly. At 650 nm, which is the upper limit for instrument #5A band, the bialkali quantum efficiency is 1%. SiPMs, which is the second choice, have as main drawback the high dark count rate, which should be reduced. The dark count rates are significantly higher than in PMTs. The lowest rates are obtained by Hamamatsu through cooling. The detectors also need further activities to achieve space qualification.

5.5 Test Procedures

Test procedures assess the fidelity, quality, and meaning of the signal delivered by the CS instrument. The proposed test measurements are:

- Radiometric calibration
- Flat-field calibration
- Spectral calibration
- Sensor's bandwidth determination
- Stray-light / MTF evaluation
- Noise assessment
- Validation measurement.

The test setup designed for testing instrument #5A includes an Optical Ground Support Equipment (OGSE) to generate the synthetic test images to be observed by the CS instrument. The OGSE provides the user with an extended control over source spectrum and image spatial texture, and with an excellent temporal stability of the emitted radiation. The OGSE emits plane-parallel beams well suited to be imaged by the input telescope of the investigated CS instrument.

Test measurements can be made either adopting the standard configuration of the CS instrument or employing an ancillary 2D array detector to be placed in the intermediate focal plane where the DMD array is located. The additional detector could be used to assess the image available for the CS digitizer (single-pixel camera equivalent) at the end of the CS sensor. The measurements performed by the 2D detector can be helpful to infer the accuracy of the image reconstruction algorithm (signal estimation procedure) as well as to detect some parameters of the telescope + spectrometer block, such as its MTF.

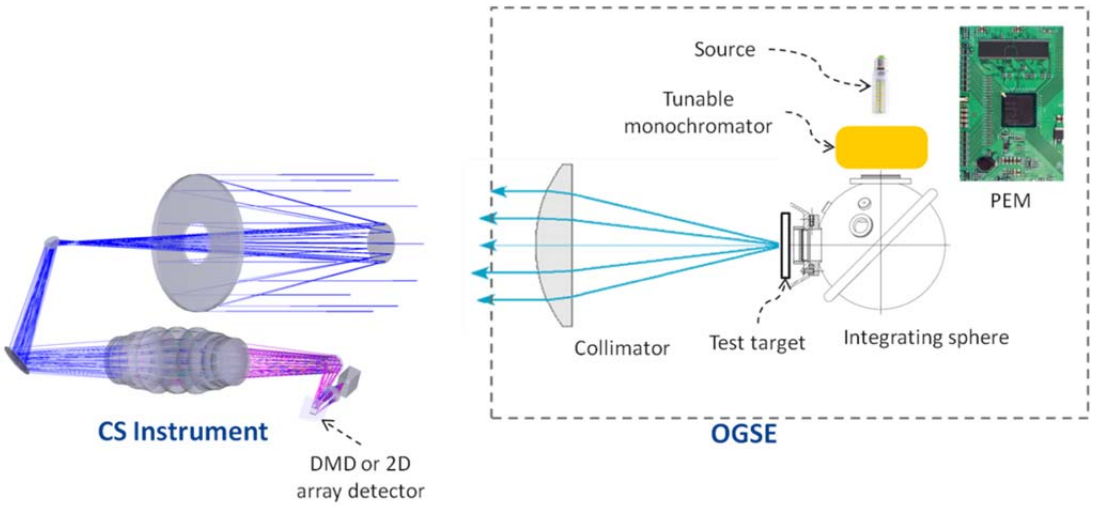

Fig. 14 – Concept #5A: general layout of the OGSE for testing the CS instrument performance.

Fig. 14 shows the basic experimental arrangement to perform the test measurements. The setup includes the aforementioned OGSE that produces the stimuli for the CS instrument and the option to use a supplementary 2D array detector in place of the DMD to execute specific additional test measurements.

6 DEVELOPMENT ROADMAP AND QUALIFICATION OF AN ENGINEERING MODEL

The roadmap for the development of an Engineering Model (EM) will consist of the following steps:

- Instrument design;
- Procurement of instrument components;
- Assembly of the main parts of instrument and final set-up;
- Development of software for data acquisition, communications and control;
- Fine tuning of modulation and reconstruction CS algorithms;
- Calibration and validation activities;
- Test in relevant environment.

A time scheduling expected for the development of an EM (single arm configuration) is reported in Table 10. Similar costs and time duration are expected for the double-arm configuration.

This EM is intended to be implemented by using components that are not space-qualified, although compatible with space qualification, and up to a level that is compatible with tests in relevant environment (thermo-mechanical and vibration tests). The development up to a space-qualified model should need the use of space qualified materials (or, in some cases, their qualification) and the overall qualification of the instrument, with consequent impact on the time scheduling.

Table 10 – Concept #5A: Roadmap for EM development.

Roadmap to Engineering Model development										
Task name	**Price (K€)**	**2016**	**2017**		**T0+6m**	**T0+12m**	**T0+18m**	**T0+24m**	**T0+30m**	**T0+36m**
Task #0: OCSTech Project										
Task #1: Instrument design	**200 - 400**									
Task #2: Procurement of instrument components	**300 - 500**									
Task #3: Assembly of the main parts of instrument and final set-up	**150 - 300**									
Task 4#: Development of software for data acquisition, comunications and control	**100 - 250**									
Task 5#: Fine tuning of modulation and reconstruction CS algorithms	**100 - 200**									
Task #6: Calibration and validation activities	**100 - 200**									
Task #7: Tests in relevant environment	**100 - 200**									

7 CONCLUSIONS

The main scope of the OCS-TECH project was to design and evaluate the performance of an instrument based on CS techniques for signal acquisition and targeting a space mission. The aim of the project was also to demonstrate a benefit in terms of volume, weight, power consumption and quality of data of a CS-based instrument with respect to the corresponding traditional one.

Starting from an initial set of 15 different “instrument concepts” proposed by the project's team for various applications in SS, PE and EO, ESA identified a slitless imaging spectrometer (Instrument #5A) operating in the UV-VIS for stellar photometry/spectroscopy as the most promising in terms of performance, budget savings as well as of applicability in near future missions. On the other hand, the high sparsity of the acquisition domain showed a good potential for obtaining a good quality of data reconstruction, yet with a high compression ratio. The detailed design led to an instrument that is pixel-limited in the entire 300 nm - 650 nm spectral range. From the point of view of data reconstruction quality, the results showed a good performance of the designed instrument. Beside the detailed design of the selected instrument, an additional configuration based on a CS two-channel architecture was studied at a preliminary level detail. This additional configuration relies on the use of all the light arriving at the DMD, both from the micromirrors in the ON and those in the OFF position, each set of micromirrors constituting a CS channel of the instrument.

The activities carried out during this project permitted to gain an in-depth understanding of the applicability of CS technology to instrumentation specifically designed for space applications. Space Science applications from UVA to TIR were found to be the most favourable for CS instrumentation, mostly due to the high degree of sparsity featured by data in this domain, which facilitates a high quality data reconstruction. On the other hand, space observation data are often characterised by very low signal energy: as a consequence, such applications often require long acquisition times and detectors working in photon-counting mode. Presently, commercial single element detectors featuring photon counting mode, large sensitive area and low noise, are available only in the UV-VIS. This circumstance reduces the spectral range presently available for implementing CS-based instrumentation for these applications. This technological limitation does not affect, of course, those applications with a higher signal level or operated from fixed platforms, which do not need photon counting detectors, but could make use of classical detectors.

Another issue worth being underlined is that, although the core components of a CS instrument are available on the market, they have been developed primarily for commercial applications and therefore they are not optimised for space applications or CS implementation.

The comparison between a CS instrument and its traditional counterpart showed some marginal benefits with reference to system budgets. Most advantages are instead provided in terms of downlink requirements and memory buffer. The knowledge gained during the project suggests that CS technology can express its best potential when the instrument retrieves information on the acquired data through the use of specific CS signal processing techniques, applied directly on-board. From this point of view, the novel information-based CS applications identified in the first part of the project, although implying a definitely higher level of risk for their development, could be very promising and, in the end, able to offer more advantages with respect to the traditional CS-approach. The dual arm architecture of the instrument #5A, which was studied during the project at a preliminary level, can be regarded as a partial example of such approach.